ACS APPLIED MATERIALS & INTERFACES

www.acsami.org
Research Article

Effective Nose-to-Brain Delivery of Blood-Brain Barrier Impermeant Anti-IL-1β Antibody via the Minimally Invasive Nasal Depot (MIND) Technique

Valentina Di Francesco, Andy J. Chua, Benjamin S. Bleier, and Mansoor M. Amiji*

Cite This: ACS Appl. Mater. Interfaces 2024, 16, 69103−69113
Read Online

ABSTRACT: Treatment of neuroinflammation and neurodegenerative diseases using biologic therapies is limited due to the blood-brain barrier (BBB). This study explores a clinically validated approach to bypass the BBB for the purposes of direct central nervous system (CNS) delivery of antibodies using the Minimally Invasive Nasal Depot (MIND) technique. Using a lipopolysaccharide (LPS)-induced mouse model of neuroinflammation, we evaluated the efficacy of MIND in delivering a BBB impermeant full-length anti-IL-1β antibody. The results demonstrated that MIND delivery resulted in a significant reduction in IL-1β levels and microglial activation in relevant brain regions, notably outperforming conventional intravenous (IV) administration. These results underscore the ability of the MIND approach to transform the treatment landscape for a range of neurodegenerative diseases by enabling the targeted delivery of otherwise BBB impermeant therapeutics.

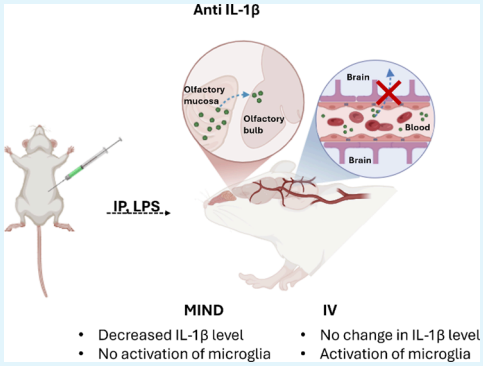

KEYWORDS: *neurodegenerative diseases, nose-to-brain delivery, neuroinflammation, CNS delivery, antibody treatment*

1. INTRODUCTION

The treatment of central nervous system (CNS) disease is hindered by the blood-brain barrier (BBB), which restricts access to the brain. Neuroinflammation, a key factor in the development and progression of neurodegenerative diseases, poses a significant challenge. In Alzheimer's disease (AD), for instance, neuroinflammation occurs before amyloid β (Aβ) deposition, highlighting its critical role in disease progression.[1] Furthermore, research suggests that neuroinflammation can trigger Parkinson's disease (PD) and depression[2] being correlated with elevated levels of inflammatory cytokines.[3] Managing neuroinflammation, therefore, becomes crucial in the effective treatment of neurodegenerative diseases.[4]

Microglia are the primary cells responsible for driving inflammatory responses within the brain.[5] Specifically, they can adopt either a homeostatic (resting) or reactive (activated) state depending on the ambient signaling.[6] When reactive, microglia secrete pro-inflammatory cytokines, which can contribute to neurodegenerative processes. In contrast, homeostatic microglia release anti-inflammatory cytokines that promote tissue repair and blood vessel growth.[4] The bacterial endotoxin lipopolysaccharide (LPS) is a potent activator of microglia. Even a single systemic exposure to LPS can trigger neuronal loss and activate microglia, leading to neurodegeneration.[7] LPS injection is a widely accepted animal model for studying neuroinflammation. Extensive research has demonstrated that LPS activates glial cells, particularly microglia, leading to the release of inflammatory cytokines and neurotoxic factors. This process triggers neuroinflammation and neuronal loss, which are key features of PD and AD.[2,8,9] Furthermore, neurotoxic factors are elevated in the microvasculature of AD patients. Specifically, increased thrombin levels damage neurons, activate microglia and astrocytes, and subsequently elevate levels of numerous inflammatory mediators.[10]

Several studies using immunotherapy in neurodegenerative disease have demonstrated the ability of antibodies to slow progression and even to improve cognitive and motor functions.[11−13] However, the primary obstacle is getting these antibodies past the protective barriers of the brain—the BBB and the blood-cerebrospinal fluid barrier—which severely limit their entry.[14] As a result, large doses are often required, increasing the risk of adverse effects.[15,16]

While techniques like focused ultrasound can temporarily open the BBB,[17−21] they also permit the passage of undesirable molecules.[22,23] Direct injection into the spinal fluid offers an alternative,[24−26] but is invasive and suboptimal for long-term, outpatient treatment. Consequently, there remains a pressing

Received: October 28, 2024
Revised: December 3, 2024
Accepted: December 4, 2024
Published: December 10, 2024

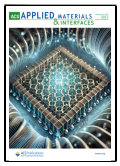

need for less invasive techniques to deliver therapeutic antibodies to the CNS.

Intranasal drug administration holds promise as a method for delivering proteins to the CNS, bypassing the BBB.[27−29] This approach has been demonstrated in preclinical and clinical studies for various molecules, from small ones such as BDNF mimetics,[30] neuropeptides,[31] insulin,[32] and calcitonin,[33] to larger antibodies like scFv[34] and full-length IgG[35,36] where detectable amounts of antibody have been identified in the rodent CNS, particularly in Alzheimer's disease models.[35,36] The prevailing theory suggests that therapeutics reach the CNS via the olfactory epithelium, and potentially the trigeminal nerve.[26,37] Nevertheless, the exact mechanism of transport through the olfactory system remains partially understood.

Despite the potential of nose-to-brain delivery, multiple clinical obstacles persist including poor nasal distribution due to the small surface area and challenging location of the olfactory mucosa, limited drug residence time due to mucociliary clearance,[38] and restricted transepithelial diffusion.[39−42] To address these issues, our lab developed the Minimally Invasive Nasal Depot (MIND) technique,[43,44] a novel nose-to-brain delivery method. MIND enables the precise endoscopic guided placement of a drug depot directly into the olfactory submucosa, thereby bypassing the BBB and minimizing systemic side effects.[43] This approach ensures optimal drug absorption, eliminates mucociliary clearance concerns, enables the use of sustained-release formulations, and is derived directly from established, safe, and validated clinical endoscopic endonasal procedures in current use.

In this study, we have investigated the utility of the MIND technique for delivering an anti-IL-1β antibody (152 kDa) to the CNS and its effectiveness in abrogating neuroinflammation in an LPS-induced murine model. The MIND administration method was compared to controls that received the antibody via intravenous (IV) injection. The goal was to assess the potential of the MIND technique as a clinically viable platform to effectively deliver large molecules such as antibodies to the CNS.

2. EXPERIMENTAL SECTION

2.1. Materials. Anti-IL-1β was purchased from) InvivoGen (San Diego). The ELISA kit for IL-1β level (R&D Systems) quantification and Abcam Cy5 Conjugation Kit (Fast) - Lightning-Link, and 4% Paraformaldehyde (PFA) solution were bought from Fisher Scientific (Fair Lawn, NJ). The drill for the surgery was obtained from Dremel (Mt. Prospect, IL) and 5−0 nylon sutures used for incision closure were purchased from MedVet International (Mettawa, IL). Anti Iba1 was purchased from Fujifilm Wako's.

2.2. Methods. *2.2.1. LPS-Induced Neuroinflammation Model.* Mice were injected intraperitoneally (IP) with 4 mg/kg *Escherichia coli* bacterial lipopolysaccharide (LPS) (serotype O111:B4, Fisher Scientific, Waltham, MA, USA), the same volume of PBS was used in the control group. Animals injected with LPS were sacrificed at different time points: i.e., 2, 6, 8, and 12 h (n = 4/group). For each time point, all the subregions of the brain were collected.

2.2.2. Quantitative Evaluations of IL-1β mRNA Transcript by qPCR. Total RNA was extracted from tissue using TRIzol (Thermo Fisher Scientific, Waltham, MA, USA) following the manufacturer's protocol. RNA was treated with RNase-free DNase I to remove contaminating genomic DNA and the purity and concentrations of extracted RNA were determined by a spectrophotometer NanoDrop 2000c (Thermo Fisher Scientific, Waltham, MA, USA). Subsequently, 2 μg of RNA was reverse transcribed to cDNA using High-Capacity cDNA Reverse Transcription Kits (Applied Biosystems, Waltham, MA, USA). Real-time qPCR was performed in the Roche Light Cycler 480 PCR system (Roche, Basel, Switzerland) with SYBR Green master mix. The sequences of gene-specific primers were IL-1β (Thermo Fisher Scientific, Waltham, MA, USA; cat # 4331182) and gapdh (Thermo Fisher Scientific, Waltham, MA, USA; cat # 4331182). The 2-ΔΔCT method was used to analyze the relative gene expression changes after normalization to the expression of gapdh.

2.2.3. Quantitative Evaluations of IL-1β Protein by ELISA. All mice in each group were euthanized 24 h postantibody injection. At each time point, blood, brain, liver, spleen, and kidneys were collected. To measure IL-1β levels in plasma, blood samples were centrifuged for 10 min at 2000g and 4 °C, with plasma being collected from the supernatant.

In the brain, the OB, HC, ST, CX, and CB were dissected. Each organ was homogenized in Cell Lysis Buffer II (Invitrogen) containing protease inhibitors and PMSF. The supernatant, containing the total protein, was collected. IL-1β levels in tissue extracts and plasma were determined using an ELISA kit following the manufacturer's instructions. The IL-1β concentrations were normalized to the tissue weight and expressed as pg IL-1β /mg tissue.

2.2.4. Anti-IL-1β Administration Using the MIND Procedure and Intravenous Administration. The procedures outlined by the Institutional Animal Care and Use Committee (IACUC) of Northeastern University were adhered to design our animal experiments. CD-1 mice (50:50 female and males, 25−30 g weight) were purchased from Charles River Laboratories (Wilmington, MA) for the study. All animals were given drinking water and diet ad libitum and maintained under standard conditions of 12 h light cycle/12 h dark cycle.

The in vivo Pluronic F127 gel depot in naïve mice was carried out using the MIND technique developed previously by our team.[45] Mice anesthetized with 2% isoflurane were placed on a stereotactic apparatus equipped with ear bars and body temperatures were maintained at 37 °C. After shaving, prepping, and draping each mouse, a 3 mm linear incision was made over the snout. The skin and soft tissue overlying the nasal bones were elevated and retracted laterally. A microscope (Vision Scientific, VS-5FZ-IFR07 Simul-Focal Trinocular Zoom Stereo) is then brought into the field for surgical illumination and magnification. Using a microdrill (Dremel Micro, model 8050-N/18), the nasal bones were thinned out, and then gently removed to expose the underlying olfactory mucosa. This exposure provided for a subcutaneous cavity in direct contact with the basolateral olfactory epithelium. The incision is then closed with nylon-6−0 sutures. Appropriate volumes of gel, composed of anti-IL-1β and Pluronic F127 at concentrations of 1, 5, and 10 mg/kg, were injected into the subcutaneous pocket using a 30g needle. After the injection, the mouse was placed on a heated pad to recover. For inducing neuroinflammation, 22 h postgel injection, a single intraperitoneal injection of LPS (4 mg/kg) was administered. Two hours later, the mice were sacrificed. As a control group, the antibody was administered either IV or subcutaneously on top of the nose (in the same position as the MIND), but in this case, the bone was not removed (surgical CTRL) Figure 2A.

2.2.5. Cy5-Labeled Anti-IL-1β Biodistribution Studies. Cy5-Anti-IL-1β was used to assess the biodistribution upon the MIND depot using a whole animal optical imaging system (IVIS). After 24 h from the treatment, the animals were euthanized, and all organs were harvested and subjected to imaging using the IVIS.

2.2.6. Semi-Qualitative Analysis of Cy5-Labeled Anti-IL-1β in the Brain Sub-Regions by Confocal Microscopy. Cy5-labeled anti-IL-1β was utilized for semiquantitative analysis of MIND depot via confocal microscopy (Carl Zeiss Microscopy GmbH, Germany). Following surgery and deposition of Pluronic F127 gel with the antibody, animals were treated for 24 h. Two hours before sacrificing the mice, neuroinflammation was induced with LPS.

After harvesting, brains were fixed in 4% paraformaldehyde (PFA) solution in PBS (Santa Cruz Biotechnology, Inc., Heidelberg, Germany) for 1 day at 4 °C, immersed in a 30% (w/v) sucrose solution in PBS for 2 days at 4 °C, embedded in OCT (optimal cutting temperature) embedding compound and frozen and stored at −80 °C until sectioning. OCT blocks were cut into 14 μm slices using a cryostat instrument. The sections were then placed on Superfrosted microscope slides (Thermo Fischer). Slides were imaged using confocal microscopy (Carl Zeiss Microscopy GmbH, Germany). All images were captured

https://doi.org/10.1021/acsami.4c18679
ACS Appl. Mater. Interfaces 2024, 16, 69103−69113

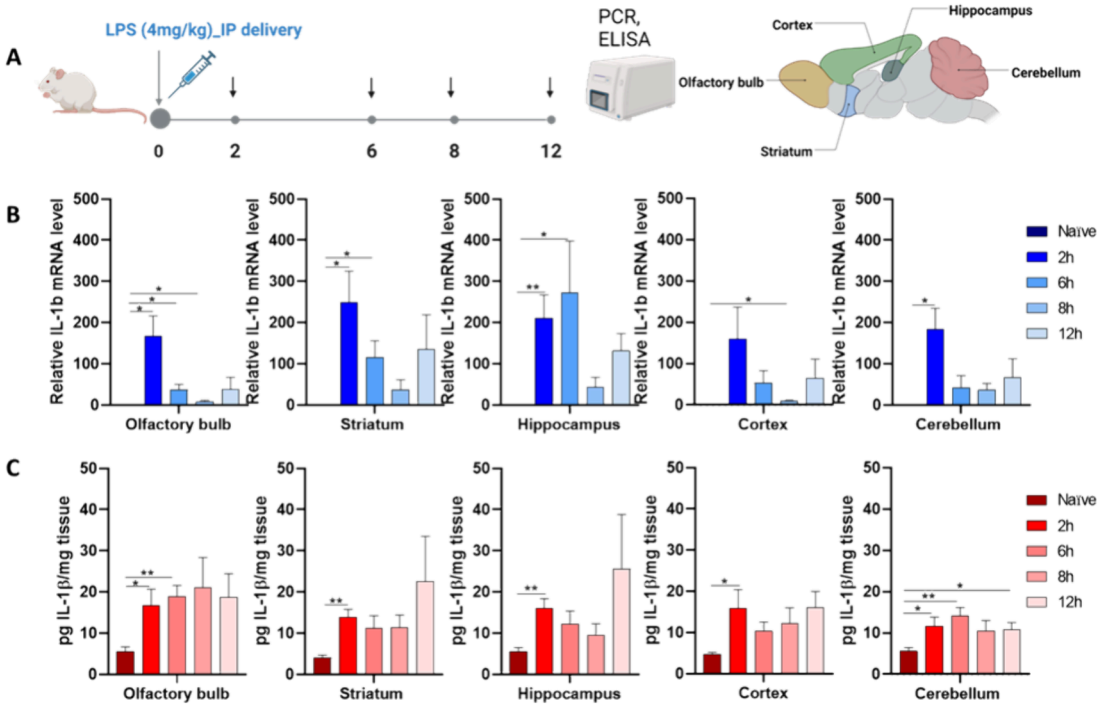

Figure 1. Neuroinflammation model: Inflammatory response in naïve mice induced by 4 mg/kg of LPS at various time points. (A) Schematic diagram showing the experimental design paradigm. (B) mRNA expression of IL-1β in distinct brain regions, including the olfactory bulb (OB), hippocampus (HC), striatum (ST), cortex (CX), and cerebellum (CR). (C) Expression of the IL-1β protein in distinct brain subregions. The data represents the mean ± SEM (n = 4), and statistical significance is denoted as follows: *P < 0.05, **P < 0.01 compared to the CTRL group.

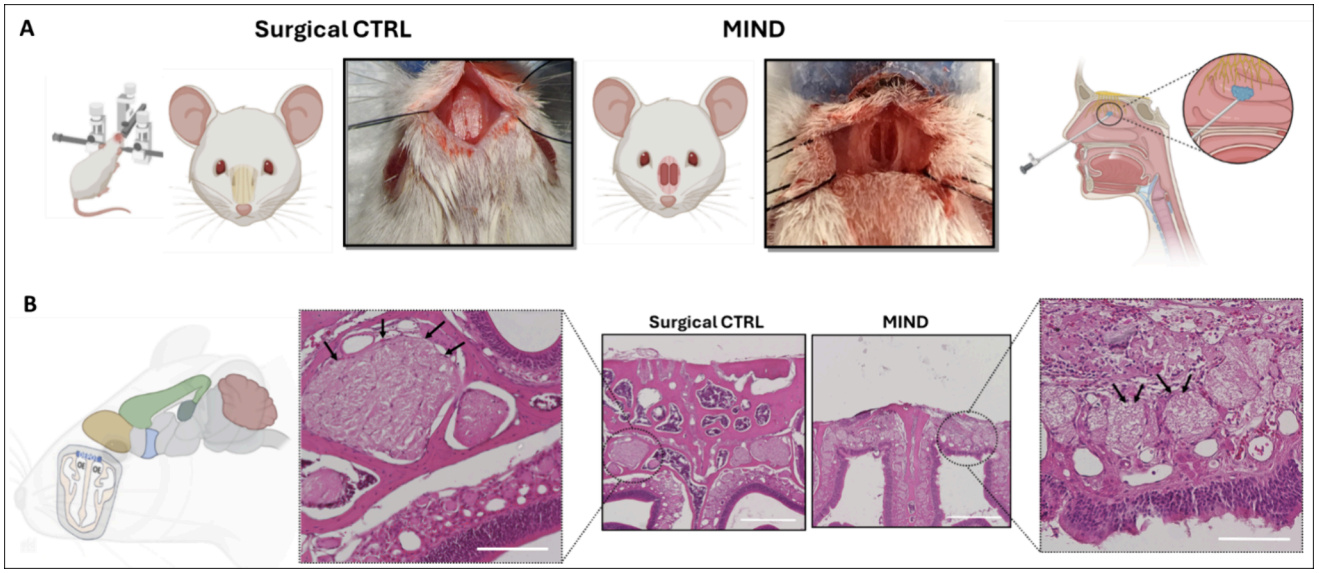

Figure 2. MIND procedure in a mouse model. (A) Mouse is placed in a stereotactic frame and the nasal bones are exposed in the surgical control (CTRL). The nasal bones are then removed in the MIND group, exposing the basolateral aspect of the olfactory epithelium. Schematic representation of the MIND within the human nasal submucosal space. (B) Histologic cross sections (H&E) sample demonstrating intact olfactory epithelium and nerve bundles (black arrows) before and after nasal bone removal (scale bar 1 mm; magnification 200 μm).

using a Zeiss LSM 880 inverted fluorescence microscopy (Carl Zeiss Microscopy GmbH, Germany) with a 10× objective. Fluorescence analysis was performed using ImageJ software. Three animals were included in each group, and five pictures were acquired for each region. The integrated density was obtained using ImageJ software.

2.2.7. Tissue Immunohistochemical Analysis. After 24h from MIND technique, mice were sacrificed, and all the brains were harvested (n = 3). Organs were kept in 4% paraformaldehyde solution in PBS at 4 °C for 24 h. After fixation, the brains were cryoprotected in sucrose 30% and embedded in OCT (optimal cutting temperature) embedding compound, and the block was snap-frozen in liquid nitrogen. OCT blocks were cut into 14-μm sagittal sections and fixed on precoated slides.

For immunofluorescence staining, the brain sections were permeabilized with 3% BSA, 0.1% Triton X-100 (Sigma T9284) in PBS (PBST) for 2h at room temperature, and subsequently incubated at 4 °C overnight with the primary antibody rabbit Ionized calcium-binding adapter molecule1 (1:250; Wako, Cat # 019-19741). The following day, brain sections were washed 3 times with PBST and incubated for 2 h at room temperature with a secondary antibody

https://doi.org/10.1021/acsami.4c18679
ACS Appl. Mater. Interfaces 2024, 16, 69103−69113

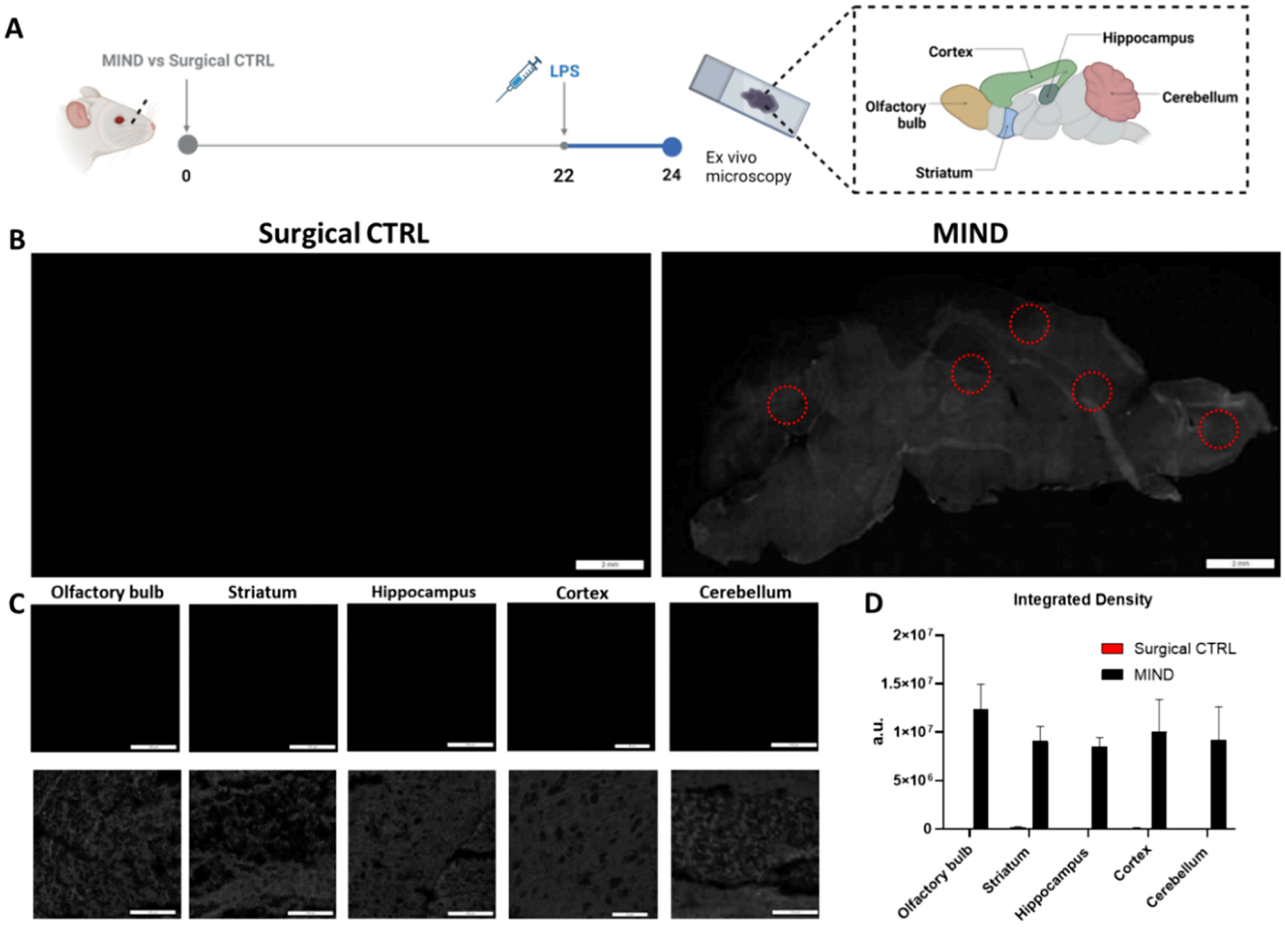

Figure 3. Semiqualitative analysis of Cy5-anti-IL-1β uptake in the brain. (A) Timeline of the experiment; (B) Sagittal confocal images are shown in grayscale, demonstrating a greater signal in MIND-treated mice. Red circles demonstrate subregions selected for detailed analysis; scale bar: 2 mm. (C) Subregion images of MINI-treated brains vs Surgical CTRL; scale bar: 100 μm. (D) Semiquantitative analysis of Cy5-Anti-IL-1β (n = 3).

conjugated to Alexa Fluor 488/594 (1:2000, goat antirabbit IgG, Alexa Fluor 488), followed by another round of PBS-T washing. Negative controls were also prepared simultaneously to detect the nonspecific binding of the secondary antibody. Nuclei were stained using DAPI. All images were captured using a Zeiss LSM 880 inverted fluorescence microscopy (Carl Zeiss Microscopy GmbH, Germany) with a 40× objective.

Three animals were used for each group, and five pictures were acquired for each region. The expression of immunoreactive proteins was analyzed by calculating the integrated density using ImageJ software.

2.2.8. Histological Analysis of Olfactory Mucosa. The surgical sites of the animals subjected to MIND were closely monitored throughout the study frame for any signs of infection, edema, or inflammation. After sacrifice, the mouse nasal cavities were opened and visually inspected for any signs of infection around the implant. Nasal tissues at the gel-nasal cavity interface were collected from the snouts of animals subjected to MIND injection upon sacrifice. The tissue samples were fixed in a% (v/v) PFA, embedded in paraffin wax, and sectioned by microtome at a thickness of 5 μm for standard histology analysis. As a control, a naïve mouse was used. Staining was done with hematoxylin and eosin (H&E) and slides were imaged with a camera-equipped microscope (Keyence BZ-X710 All-in-One Fluorescence Microscope, Itasca, IL) for the qualitative analysis of the gross morphology of tissues at the interface of implant and nasal cavity.

2.2.9. Statistical Data Analysis. The experiments were conducted using either 3 or 6 samples, and the resulting experimental data is presented as mean ± SEM. Statistical significance was evaluated using a t test, and the analysis was performed using GraphPad Prism.

3. RESULTS AND DISCUSSION

3.1. Results. *3.1.1. LPS-Induced Neuroinflammation Model Development and Characterization.* To determine the optimal time point for inducing inflammation in various brain regions, we measured the gene and protein expressions of IL-1β at 2, 6, 8, and 12 h (Figure 1A).

Robust endotoxin-induced inflammatory responses were observed. After LPS exposure, a peak in IL-1β gene expression was noted at 2 h, particularly in the olfactory bulb (OB) 167 ± 49, hippocampus (HC) 210 ± 56, striatum (ST) 249 ± 76, cortex (CX) 159 ± 77, and cerebellum (CR) 184 ± 50 compared to naïve animals (Figure 1B). This peak was followed by a gradual reduction in expression over time.

Expression levels of IL-1β protein (Figure 1C) were consistently elevated across all time points, with the greatest degree of interval change seen at the 2-h mark in most brain subregions. This time point was thus selected for evaluating induced neuroinflammation in the mice.

3.1.2. Histology. We began with a safety evaluation of the MIND technique (Figure 2), which is described further in the methods section. We observed that all mice tolerated the procedure well and remained healthy throughout the entire experiment, as demonstrated by parameters such as body weight and activity levels.

Our observations showed no significant changes in the tissue histology of treated animals compared to the intact histology of untreated controls. The absence of any notable histological signs

https://doi.org/10.1021/acsami.4c18679
ACS Appl. Mater. Interfaces 2024, 16, 69103−69113

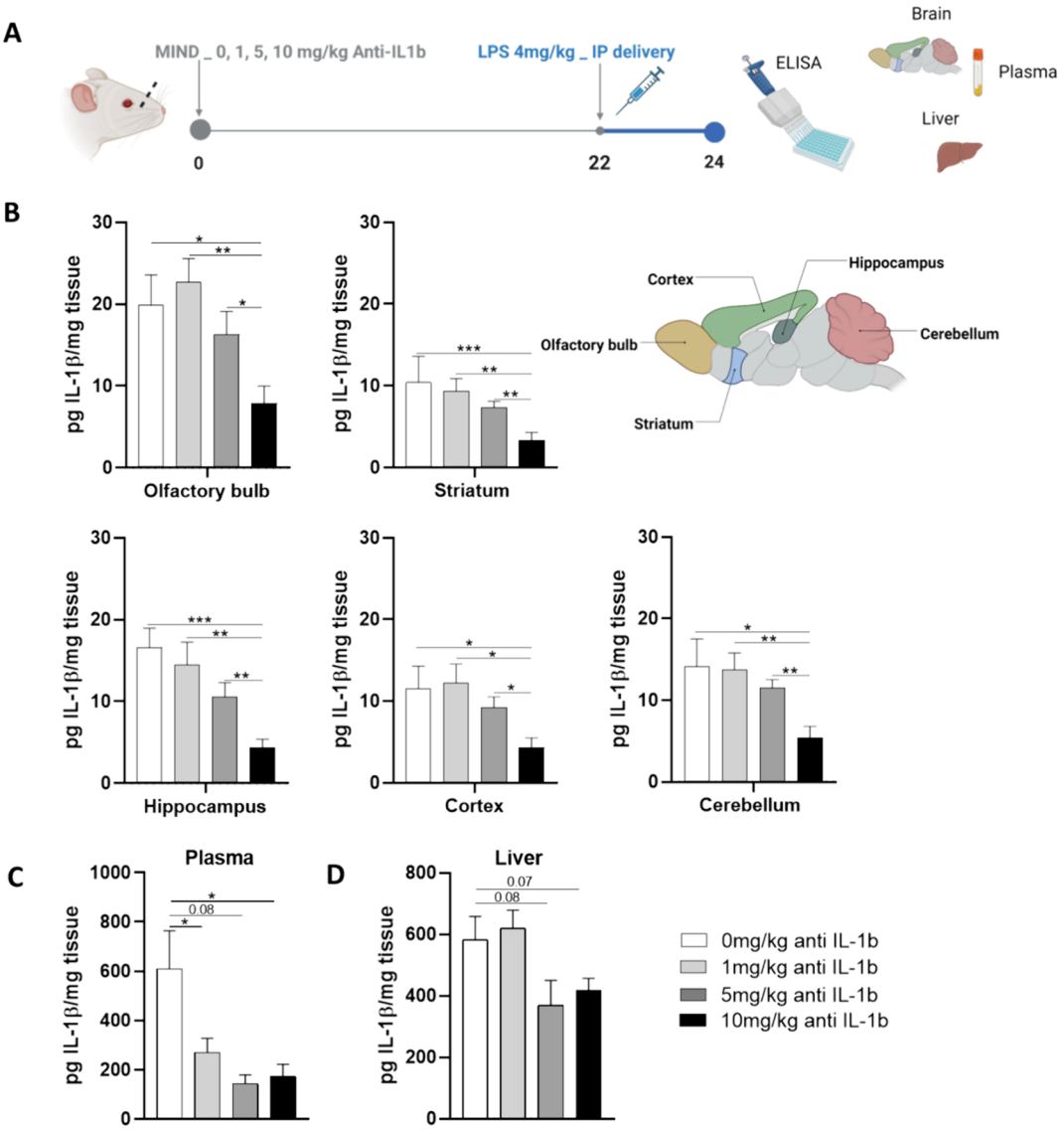

Figure 4. Dose−response relationship. Reduction of IL-1β protein after antibody treatment. (A) Schematic of the experiment design. (B) IL-1β levels after the treatment with different doses of the antibody, e.g. 0 to 10 mg/kg, in the different subregions of the brain (C) IL-1β levels after the treatment with different doses of the antibody, e.g., 0 to 10 mg/kg, in plasma. (D) IL-1β levels after the treatment with different doses of the antibody, e.g., 0 to 10 mg/kg, in the liver. The data are described as the mean ± SEM (n = 6). *P < 0.05, **P < 0.01 ***P < 0.001.

of adverse tissue reactions confirmed the safety of this surgical method (Figure 2B). In our previous work with rats, we also demonstrated the reproducibility of the MIND surgery and found no alterations in the mucosa of the animals subjected to the procedure.[44,46]

3.1.3. Qualitative Analysis of Cy5-Labeled Anti-IL-1β in the Brain. Following the histology analysis, we evaluated the efficacy of a 10 mg/kg dose of anti-IL-1β administered 24 h postinjection of the antibody via imaging. To quantify antibody uptake, Cy5-conjugated anti-IL-1β was employed. Neuroinflammation was induced in mice via LPS injection 2 h before euthanasia. Brains were then collected for ex vivo imaging using IVIS (Figure S1). Compared to naive controls (CTRL) an surgical controls, mice subjected to MIND exhibited significantly stronger fluorescence signals (Figure S1), indicating antibody penetration into the inflamed brain region. Notably, Cy5-conjugated anti-IL-1β was also detected in the liver, with a higher signal observed in the surgical control group as compared to the MIND group.

Confocal microscopy, utilizing a 640 nm laser, was employed to obtain Z-stacks and perform image stitching, enabling the reconstruction of complete sagittal brain slices. Quantitative analysis of integrated density (Figure 3A−D) demonstrated a diffuse increase in signal intensity throughout the brains of the MIND group compared to the surgical control group. This observation was corroborated by representative images, and further confirmed by analysis of specific brain subregions.

3.1.4. Anti-IL-1β Delivery in the Brain: The Neuroinflammation Model. To determine the most suitable antibody dose for pretreatment prior to induction of neuroinflammation, a dose−response study was conducted. The antibody was first dissolved in a thermosensitive gel (26% w/v Pluronic F127 gel), which did not interfere with its activity (Figure S2). Mice in the MIND treatment group were pretreated with 0, 1, 5, or 10 mg/kg of the antibody as a gel depot and monitored for 24 h. Neuroinflammation was then induced by LPS 2 h before euthanasia, and IL-1β levels were quantified in brain, plasma, and liver tissues (Figure 4A).

https://doi.org/10.1021/acsami.4c18679
ACS Appl. Mater. Interfaces 2024, 16, 69103−69113

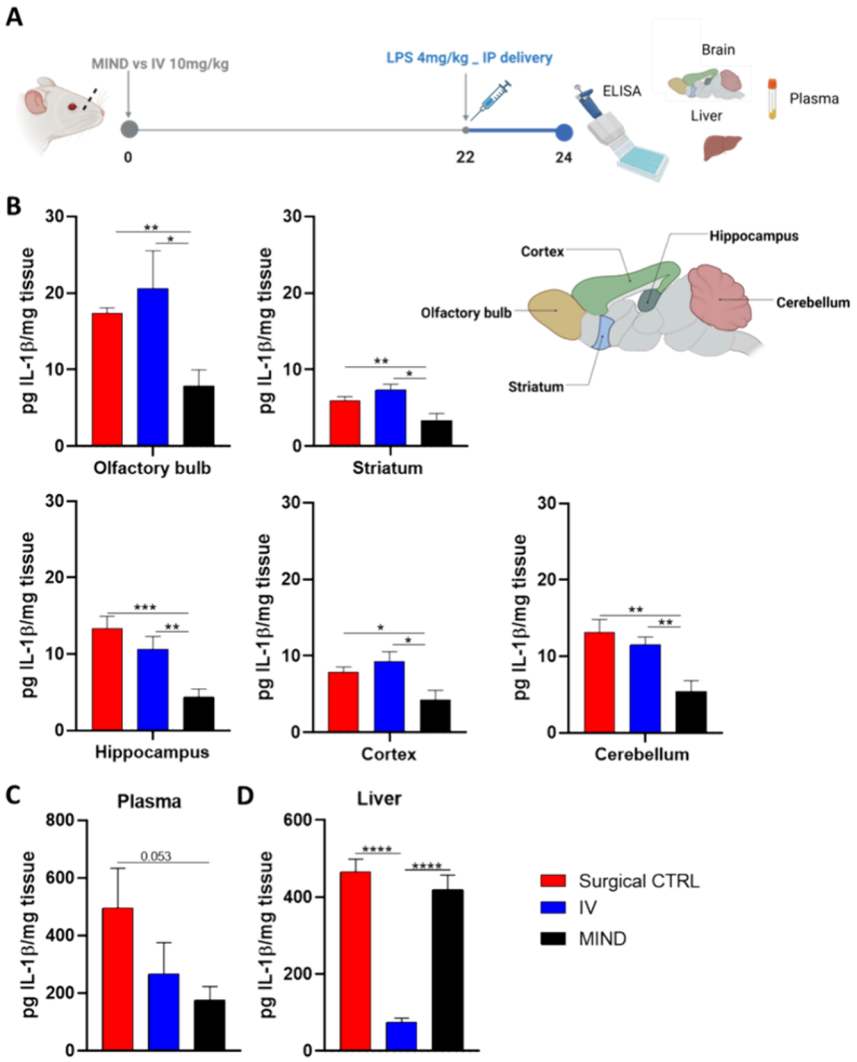

Figure 5. Comparison of different routes. Reduction of IL-1β protein after antibody treatment. (A) Timeline of the experiment; (B) IL-1β levels after treatment with 10 mg/kg of antibody in the different regions of the brain (olfactory bulb, hippocampus, striatum, cortex, and cerebellum). (C) IL-1β levels after treatment with 10 mg/kg of antibody in the liver. (D) IL-1β levels after treatment with 10 mg/kg of antibody in plasma. The data are described as the mean ± SEM ($n = 6$). *$P < 0.05$, **$P < 0.01$, *** $P < 0.001$.

Results indicated a dose-dependent response trend (Figure 4B), with the 10 mg/kg concentration demonstrating the most significant reduction in IL-1β protein expression. Specifically, in the brain, the 10 mg/kg group exhibited substantially lower IL-1β levels compared to the 0 mg/kg group in all regions: OB 7.8 ± 2.1 vs 19.9 ± 3.7, HC 4.3 ± 1.0 vs 16.6 ± 2.3, ST 3.4 ± 0.9 vs 10.4 ± 3.1, CX 4.3 ± 1.2 vs 11.6 ± 2.7, and CB 5.4 ± 1.4 vs 14.2 ± 3.3. Interestingly, a systemic reduction of IL-1β was observed in plasma across all tested concentrations. However, no significant changes were seen in IL-1β levels in the liver, regardless of the concentration used (Figure 4C,D).

3.1.5. Comparison of the Effects of Identical Antibody Concentrations Delivered via Different Routes. After determining 10 mg/kg as the optimal treatment concentration, we conducted an experiment to compare the effectiveness of different delivery methods. Specifically, we aimed to characterize the reduction of IL-1β in the CNS using the MIND technique, surgical control (without olfactory mucosa exposure), and intravenous (IV) administration. The same timeline was followed for all groups (Figure 5A).

At 24 h post-treatment, various CNS subregions (olfactory bulb, hippocampus, striatum, frontal cortex, and cerebellum) were isolated, and IL-1β concentrations were quantified using ELISA (Figure 5B). Mice subjected to the MIND technique showed significantly higher protein reduction in all regions than in the surgical control and IV groups. Specifically, the MIND group exhibited a significant decrease in IL-1β levels compared to the surgical control and IV group: 55% in the striatum, 52% in the cortex, 46% in the cerebellum, 44% in the olfactory bulb, and 38% in the hippocampus.

Additionally, we assessed systemic effects in plasma and liver (Figure 5C,D). Both the MIND and IV groups showed reduced IL-1β protein expression in the plasma. However, in the liver, only the IV group significantly reduced inflammation ($p < 0.0001$ compared to the other 2 groups). One possible reason could be that in the MIND group, a higher proportion of anti-IL-1β was taken up into the CNS, with less circulating in the peripheral circulation. Alternatively, systemic absorption of antibody when administered via MIND is through the subcutaneous route, which may lead to a reduced amount

https://doi.org/10.1021/acsami.4c18679
ACS Appl. Mater. Interfaces 2024, 16, 69103−69113

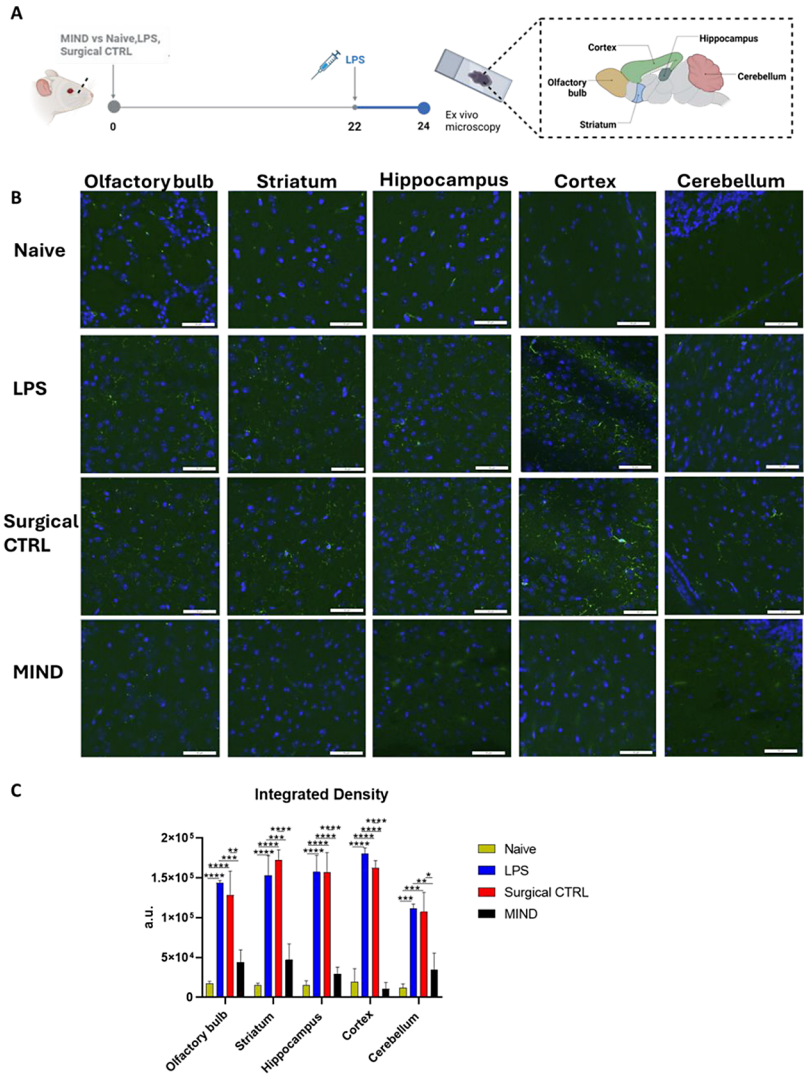

Figure 6. Semiquantitative analysis of IBA-1 in the brain. (A) Timeline of the experiment; (B) representative pictures of the IBA-1 expression in the neuro-inflamed model mouse. Immunostaining of IBA-1 protein (depicted in green) conducted in various brain regions, olfactory bulb, hippocampus, striatum, cortex, and cerebellum, comparing the Naïve, LPS, Surgical CTRL group against the MIND group (scale bar 100 um): (C) Semiquantitative analysis of IBA-1 (n = 3).

reaching the liver compared to when antibodies were delivered by IV injection.

3.1.6. Microglial Activation and Response to Anti-IL-1β Delivered. In the LPS-induced neuroinflammation mouse model, microglial response to toxic stimuli has been well-documented.[47] Our focus primarily lies on the olfactory bulb, a key region involved in drug diffusion using the MIND technique, as well as the hippocampus, striatum, cortex, and cerebellum, which are implicated in neurodegenerative diseases due to inflammation. Microglial activation, indicated by Iba1 immunoreactive staining in various brain regions post-LPS injection, signifies the presence of inflammation (Figure 6A,B).

As observed in the calculation of integrated density and representative images (Figure 6C), microglial reactivity increased in the LPS and Surgical CTRL groups as compared to the naïve group. The increase in integrated density was particularly striking, with an 8-fold increase in the olfactory bulb, 10.5-fold in the striatum, 10.3-fold in the hippocampus, 9-fold in the cortex, and 9.3-fold in the cerebellum compared to the naive group.

Pretreatment with anti-IL-1β via the MIND technique significantly attenuated this LPS-induced microglial reactivity in all brain regions ($p < 0.01$). The reduction in integrated density in the MIND group compared to the LPS and surgical control groups was approximately 30% in the olfactory bulb, striatum, and cerebellum. The hippocampus and cortex showed 18.6 and 6.3% reductions, respectively.

3.2. Discussion. Currently, effective treatment strategies for neurodegenerative diseases remain elusive. New candidate drugs and strategies with improved clinical therapeutic effects are urgently needed but face delivery limitations due to the BBB.

Our study provides promising evidence for the use of anti-IL-1β to modulate neuroinflammation following delivery using the MIND technique. The ability to deliver anti-IL-1β, an antibody with a molecular weight of 152 kDa, further suggests the broader applicability of MIND for a host of biological agents. By employing the intranasal route, we demonstrated direct delivery to the brain while minimizing systemic uptake into peripheral organs such as the liver.

LPS, an endotoxin from the cell wall of Gram-negative bacteria, is commonly used to model cerebral inflammation,

https://doi.org/10.1021/acsami.4c18679
ACS Appl. Mater. Interfaces 2024, 16, 69103−69113

Table 1. Illustrative Examples of Antibody-Based Immunotherapy Clinical Trials in the Treatment of Neurodegenerative Diseases

name	disease	role	clinical trial registation	route of administation	molecular weight (kDa)
Donanemab	Alzheimer	Aβ monoclonal antibody	phase III, recruiting (NCT05508789)	IV	145
E2814 vs Lecanemab	Alzheimer	antimicrotubule-binding region (MTBR) tau antibody vs Aβ monoclonal antibody	phase III, recruiting (NCT05269394)	IV	150 Vs 150
Remternetug	Alzheimer	Aβ monoclonal antibody	phase III, recruiting (NCT05463731)	IV	145
Aducanumab	Alzheimer	Aβ monoclonal antibody	phase III, recruiting (NCT05310071)	IV	146
Gantenerumab	Alzheimer	Aβ fibril monoclonal antibody	phase III, active (NCT05256134)	SQ	146
Prasinezumab	Parkinson	monoclonal antibody directed against aggregated α-syn−(C-terminus)	phase II, active- not recruiting (NCT03100149), recruiting (NCT04777331)	IV	150
Cinpanemab	Parkinson	monoclonal antibody directed against aggregated α-syn−(N-terminus)	phase II, terminated (NCT03318523)	IV	147
Lu AF82422	Parkinson and Multiple System Atrophy (AMULET)	monoclonal antibody directed against all forms of α-syn−(C- and N- terminus)	phase I, terminated (NCT03611569): phase I, recruiting (NCT05104476)	IV	150

with extensive literature demonstrating its ability to induce neuroinflammation in animal models.[48−51] Our results confirmed that intraperitoneal LPS injection induced neuroinflammatory responses, as represented both by the increased level of IL-1β and the activation of microglia in the brain after 2 h (Figure 1 A).

Immunotherapy for neurodegenerative diseases has rapidly advanced in recent years, moving from initial concepts to numerous clinical trials.[52−54] The FDA has approved several antibodies for neurodegenerative disease, including aducanumab (Aduhelm, Biogen), lecanemab (Leqembi, Eisai, and Biogen), and donanemab (Kinsula, Eli Lilly), with others such as gantenerumab and remternetug currently in the pipeline (Table 1).[54−57]

However, despite the promise of these antibody treatments, significant challenges remain. Due to their large molecular weight, the BBB poses a significant obstacle to achieving effective antibody concentrations in the CNS, which limits the clinical impact of these drugs. For example, recently approved drugs for AD such as lecanemab and aducanumab were found to have concerning side effects such as brain swelling in many patients, while only achieving a 27% reduction in cognitive decline. These suboptimal outcomes were attributable at least in part to their intravenous delivery route and the need for high doses to overcome limited drug amounts crossing the BBB.[55] These issues highlight the urgent need for new delivery approaches to unlock the full potential of immunotherapy in neurodegenerative diseases, and effective ways to transport antibodies across the BBB must be sought.

Intranasal drug delivery has emerged as a promising approach, with clinical and preclinical studies demonstrating its safety and efficacy.[58−61] The MIND technique, developed within this context, leverages the unique anatomical connection between the olfactory nasal mucosa and the CNS, offering a direct and rapid route for drug delivery to the brain. This approach circumvents the BBB, minimizing systemic exposure[43] and enhancing targeted therapeutic effects.

Unlike standard intranasal delivery, MIND exploits the trans-olfactory pathway, by directly depositing drugs into the olfactory submucosa (Figure 2A). This ensures precise and highly efficient delivery of the entire dose, overcoming challenges like mucociliary clearance and limited trans-epithelial diffusion that often plague traditional intranasal methods. By bypassing these obstacles, MIND enhances the dose uniformity and overall effectiveness of drug delivery to the brain.[43]

Our previous work demonstrated that this technique is safe, well tolerated by rats, and did not induce local mucosal trauma.[44] In agreement with previous findings, histologic analysis of the depot site (Figure 2B) did not demonstrate inflammation, necrosis, or neuropathic changes to the olfactory nerves.

As compared to the surgical control and IV administration, MIND delivery of anti-IL-1β significantly increased antibody diffusion through the CNS, leading to greater therapeutic efficacy (Figure 5) which is in concordance with our previous work.[43] The presence of the nasal bone in surgical controls prevented contact of the depot with the olfactory mucosa, resulting in no reduction of inflammation (Figure 5B). Control mice receiving antibodies via the IV route (which represents the current clinical standard), exhibited no reduction in brain inflammation at the chosen dose (10 mg/kg). This finding is consistent with the limitations posed by the BBB. Typically, this barrier formed by endothelial cells and tight junctions, allows only small, lipid-soluble drugs (with a molecular weight below 0.6 kDa) to pass through.[62−64] Existing research shows that less than 1% of peripherally administered antibodies reach the brain, even in neurodegenerative diseases where increased BBB permeability might be expected.[18,65−68] Interestingly, IV administration did show a higher decrease in IL-1β levels within the liver as compared to the MIND group (Figure 5D). This suggests that MIND delivery not only allows for BBB penetration but also minimizes systemic exposure, an important feature when dealing with therapeutics which could induce off-target systemic side effects.

Our brain subregion analysis revealed that the most pronounced anti-inflammatory effect occurred within the hippocampus (MIND 4.9 $\pm$ 1.0 vs Surgical CTRL 12.9 $\pm$ 1.6 vs IV 11.8 $\pm$ 1.7). This brain region, a key component of the limbic system, plays a pivotal role in memory, learning, and emotions. Its involvement in various neurodegenerative diseases, including Alzheimer's Disease has been well-established, making it a crucial target for therapeutic interventions.[69,70]

Given that LPS induces neuroinflammation, we also examined microglial activity in relevant specific brain regions. Compared to the control group, we observed heightened microgliosis in both LPS-treated and surgical control groups. However, in the

https://doi.org/10.1021/acsami.4c18679
ACS Appl. Mater. Interfaces 2024, 16, 69103−69113

MIND group, the anti-IL-1β antibody significantly suppressed LPS-induced microglial activation (Figure 6).

The present study successfully established a LPS-induced mouse model to investigate neuroinflammation, characterized by elevated levels of IL-1β in both the CNS and peripheral tissues. The MIND technique demonstrated the superiority over both traditional IV administration and surgical controls in its ability to deliver therapeutically effective levels of anti-IL-1β antibodies to reduce IL-1β levels in crucial brain regions like the hippocampus and suppress microglial activation while sparing peripheral organs. The mechanism behind this success lies in MIND's ability to bypass the BBB, a major obstacle in drug delivery to the CNS, as further evidenced by the detection of labeled antibody within multiple important brain subregions including the hippocampus. Given that the studied delivery method is directly derived from established endoscopic clinical procedures, these results suggest that MIND could serve as a clinically viable platform for delivering a range of therapeutic antibodies directly to CNS, opening new avenues for treating both neuroinflammatory and neurodegenerative diseases while limiting systemic side effects.

4. CONCLUSIONS

Our study suggests that the MIND technique has the potential to revolutionize the treatment landscape for neurodegenerative diseases by overcoming the limitations of traditional drug delivery methods, leading to a paradigm shift in the treatment of CNS diseases. In addition, the success of MIND technique in delivering large molecules into the CNS could pave the way for the continued development of novel therapeutics with a large molecular weight, broadening the spectrum of viable drug candidates to treat CNS diseases, and enabling clinicians to have more options to manage this group of conditions that are set to become an increasing global health burden.

However, future studies are needed to investigate whether antibody presence following MIND delivery could elicit long-term adaptive responses in the body. Potential immune tolerance or other adaptive changes may impact the durability of treatment effects, underscoring the importance of examining these factors for sustained therapeutic efficacy.

■ ASSOCIATED CONTENT

Data Availability Statement

Data will be made available upon request.

Supporting Information

The Supporting Information is available free of charge at https://pubs.acs.org/doi/10.1021/acsami.4c18679.

Qualitative analysis of Cy5-IL-1β uptake in distinct anatomical regions and the stability of the antibody in Pluronic F127 thermogeling system (PDF)

■ AUTHOR INFORMATION

Corresponding Author

Mansoor M. Amiji − *Department of Pharmaceutical Sciences, School of Pharmacy and Pharmaceutical Sciences, Northeastern University, Boston, Massachusetts 02115, United States; Department of Chemical Engineering, College of Engineering, Northeastern University, Boston, Massachusetts 02115, United States;* orcid.org/0000-0001-6170-881X; Email: m.amiji@northestern.edu

Authors

Valentina Di Francesco − *Department of Pharmaceutical Sciences, School of Pharmacy and Pharmaceutical Sciences, Northeastern University, Boston, Massachusetts 02115, United States; Department of Otolaryngology, Massachusetts Eye and Ear Infirmary, Harvard Medical School, Boston, Massachusetts 02114, United States*

Andy J. Chua − *Department of Pharmaceutical Sciences, School of Pharmacy and Pharmaceutical Sciences, Northeastern University, Boston, Massachusetts 02115, United States; Department of Otorhinolaryngology−Head and Neck Surgery, Sengkang General Hospital, Singapore 544886, Singapore*

Benjamin S. Bleier − *Department of Otolaryngology, Massachusetts Eye and Ear Infirmary, Harvard Medical School, Boston, Massachusetts 02114, United States*

Complete contact information is available at: https://pubs.acs.org/10.1021/acsami.4c18679

Author Contributions

Conceptualization: V.D.F., M.A., and B.B.; methodology: V.D.F. and A.C.; investigation: V.D.F., A.C., M.A., and B.B.; supervision: M.A. and B.B.; writing—original draft: V.D.F., M.A., and B.B.; writing—review and editing: V.D.F., A.C., M.A., and B.B.

Notes

The authors declare no competing financial interest.

■ ACKNOWLEDGMENTS

The authors acknowledge the assistance provided by Biania Fan and Philip Seifert at the SERI Morphology Core, Schepens Eye Research Institute of Massachusetts Eye and Ear Infirmary (Boston, MA) for the assistance provided with the hematoxylin and eosin (H&E) staining. The authors acknowledge also the Institute for Chemical Imaging of Living Systems at Northeastern University for consultation and imaging support.

■ REFERENCES

(1) Calsolaro, V.; Edison, P. Neuroinflammation in Alzheimer's disease: current evidence and future directions. *Alzheimer's Dementia* **2016**, *12* (6), 719−732.

(2) Guo, M.; Wang, J.; Zhao, Y.; Feng, Y.; Han, S.; Dong, Q.; Cui, M.; Tieu, K. Microglial exosomes facilitate α-synuclein transmission in Parkinson's disease. *Brain* **2020**, *143* (5), 1476−1497.

(3) Husain, M. I.; Strawbridge, R.; Stokes, P. R.; Young, A. H. Anti-inflammatory treatments for mood disorders: systematic review and meta-analysis. *Journal of Psychopharmacology* **2017**, *31* (9), 1137−1148.

(4) Gouveia, F.; Camins, A.; Ettcheto, M.; Bicker, J.; Falcao, A.; Cruz, M. T.; Fortuna, A. Targeting brain Renin-Angiotensin System for the prevention and treatment of Alzheimer's disease: Past, present and future. *Ageing Research Reviews* **2022**, *77*, No. 101612.

(5) Fakhoury, M. Microglia and astrocytes in Alzheimer's disease: implications for therapy. *Current neuropharmacology* **2018**, *16* (5), 508−518.

(6) Paolicelli, R. C.; Sierra, A.; Stevens, B.; Tremblay, M.-E.; Aguzzi, A.; Ajami, B.; Amit, I.; Audinat, E.; Bechmann, I.; Bennett, M.; et al. Microglia states and nomenclature: A field at its crossroads. *Neuron* **2022**, *110* (21), 3458−3483.

(7) Masocha, W. Systemic lipopolysaccharide (LPS)-induced microglial activation results in different temporal reduction of CD200 and CD200 receptor gene expression in the brain. *Journal of neuroimmunology* **2009**, *214* (1−2), 78−82.

(8) Kobayashi, K.; Imagama, S.; Ohgomori, T.; Hirano, K.; Uchimura, K.; Sakamoto, K.; Hirakawa, A.; Takeuchi, H.; Suzumura, A.; Ishiguro, N.; et al. Minocycline selectively inhibits M1 polarization of microglia. *Cell Death Dis.* **2013**, *4* (3), No. e525.

(9) Walker, F. R.; Beynon, S. B.; Jones, K. A.; Zhao, Z.; Kongsui, R.; Cairns, M.; Nilsson, M. Dynamic structural remodelling of microglia in health and disease: a review of the models, the signals and the mechanisms. *Brain, behavior, and immunity* **2014**, *37*, 1−14.
(10) Zlokovic, B. V. Neurovascular pathways to neurodegeneration in Alzheimer's disease and other disorders. *Nat. Rev. Neurosci.* **2011**, *12* (12), 723−738.
(11) Boutajangout, A.; Ingadottir, J.; Davies, P.; Sigurdsson, E. M. Passive immunization targeting pathological phospho-tau protein in a mouse model reduces functional decline and clears tau aggregates from the brain. *Journal of neurochemistry* **2011**, *118* (4), 658−667.
(12) Chai, X.; Wu, S.; Murray, T. K.; Kinley, R.; Cella, C. V.; Sims, H.; Buckner, N.; Hanmer, J.; Davies, P.; O'Neill, M. J.; et al. Passive immunization with anti-Tau antibodies in two transgenic models: reduction of Tau pathology and delay of disease progression. *J. Biol. Chem.* **2011**, *286* (39), 34457−34467.
(13) Yanamandra, K.; Kfoury, N.; Jiang, H.; Mahan, T. E.; Ma, S.; Maloney, S. E.; Wozniak, D. F.; Diamond, M. I.; Holtzman, D. M. Anti-tau antibodies that block tau aggregate seeding in vitro markedly decrease pathology and improve cognition in vivo. *Neuron* **2013**, *80* (2), 402−414.
(14) Engelhardt, B.; Sorokin, L. The blood−brain and the blood−cerebrospinal fluid barriers: function and dysfunction. In *Seminars in immunopathology*; Springer, 2009; Vol. *31*, pp 497−511.
(15) Taal, W.; Oosterkamp, H. M.; Walenkamp, A. M.; Dubbink, H. J.; Beerepoot, L. V.; Hanse, M. C.; Buter, J.; Honkoop, A. H.; Boerman, D.; de Vos, F. Y.; et al. Single-agent bevacizumab or lomustine versus a combination of bevacizumab plus lomustine in patients with recurrent glioblastoma (BELOB trial): a randomised controlled phase 2 trial. *Lancet Oncol.* **2014**, *15* (9), 943−953.
(16) Sevigny, J.; Chiao, P.; Bussière, T.; Weinreb, P. H.; Williams, L.; Maier, M.; Dunstan, R.; Salloway, S.; Chen, T.; Ling, Y.; et al. The antibody aducanumab reduces Aβ plaques in Alzheimer's disease. *Nature* **2016**, *537* (7618), 50−56.
(17) Yu, Y. J.; Zhang, Y.; Kenrick, M.; Hoyte, K.; Luk, W.; Lu, Y.; Atwal, J.; Elliott, J. M.; Prabhu, S.; Watts, R. J.; et al. Boosting brain uptake of a therapeutic antibody by reducing its affinity for a transcytosis target. *Sci. Transl. Med.* **2011**, *3* (84), 84ra44.
(18) Yu, Y. J.; Watts, R. J. Developing therapeutic antibodies for neurodegenerative disease. *Neurotherapeutics* **2013**, *10* (3), 459−472.
(19) Jordão, J. F.; Ayala-Grosso, C. A.; Markham, K.; Huang, Y.; Chopra, R.; McLaurin, J.; Hynynen, K.; Aubert, I. Antibodies targeted to the brain with image-guided focused ultrasound reduces amyloid-β plaque load in the TgCRND8 mouse model of Alzheimer's disease. *PloS one* **2010**, *5* (5), No. e10549.
(20) Chen, C. C.; Sheeran, P. S.; Wu, S.-Y.; Olumolade, O. O.; Dayton, P. A.; Konofagou, E. E. Targeted drug delivery with focused ultrasound-induced blood-brain barrier opening using acoustically-activated nanodroplets. *J. Controlled Release* **2013**, *172* (3), 795−804.
(21) Fan, C.-H.; Lin, W.-H.; Ting, C.-Y.; Chai, W.-Y.; Yen, T.-C.; Liu, H.-L.; Yeh, C.-K. Contrast-enhanced ultrasound imaging for the detection of focused ultrasound-induced blood-brain barrier opening. *Theranostics* **2014**, *4* (10), 1014.
(22) Rapoport, S. I.; Bachman, D. S.; Thompson, H. K. Chronic effects of osmotic opening of the blood-brain barrier in the monkey. *Science* **1972**, *176* (4040), 1243−1245.
(23) Kovacs, Z. I.; Kim, S.; Jikaria, N.; Qureshi, F.; Milo, B.; Lewis, B. K.; Bresler, M.; Burks, S. R.; Frank, J. A. Disrupting the blood−brain barrier by focused ultrasound induces sterile inflammation. *Proc. Natl. Acad. Sci. U. S. A.* **2017**, *114* (1), E75−E84.
(24) Calias, P.; Banks, W. A.; Begley, D.; Scarpa, M.; Dickson, P. Intrathecal delivery of protein therapeutics to the brain: a critical reassessment. *Pharmacology & therapeutics* **2014**, *144* (2), 114−122.
(25) Ineichen, B. V.; Kapitza, S.; Bleul, C.; Good, N.; Plattner, P. S.; Seyedsadr, M. S.; Kaiser, J.; Schneider, M. P.; Zörner, B.; Martin, R.; et al. Nogo-A antibodies enhance axonal repair and remyelination in neuro-inflammatory and demyelinating pathology. *Acta Neuropathol.* **2017**, *134* (3), 423−440.
(26) Pizzo, M. E.; Wolak, D. J.; Kumar, N. N.; Brunette, E.; Brunnquell, C. L.; Hannocks, M. J.; Abbott, N. J.; Meyerand, M. E.; Sorokin, L.; Stanimirovic, D. B.; et al. Intrathecal antibody distribution in the rat brain: surface diffusion, perivascular transport and osmotic enhancement of delivery. *J. Physiol.* **2018**, *596* (3), 445−475.
(27) Sakane, T.; Akizuki, M.; Taki, Y.; Yamashita, S.; Sezaki, H.; Nadai, T. Direct drug transport from the rat nasal cavity to the cerebrospinal fluid: the relation to the molecular weight of drugs. *J. Pharm. Pharmacol.* **1995**, *47* (5), 379−381.
(28) Thorne, R.; Hanson, L.; Ross, T.; Tung, D.; Frey, W., II Delivery of interferon-β to the monkey nervous system following intranasal administration. *Neuroscience* **2008**, *152* (3), 785−797.
(29) Lochhead, J. J.; Thorne, R. G. Intranasal delivery of biologics to the central nervous system. *Advanced drug delivery reviews* **2012**, *64* (7), 614−628.
(30) Simmons, D. A.; Belichenko, N. P.; Yang, T.; Condon, C.; Monbureau, M.; Shamloo, M.; Jing, D.; Massa, S. M.; Longo, F. M. A small molecule TrkB ligand reduces motor impairment and neuropathology in R6/2 and BACHD mouse models of Huntington's disease. *J. Neurosci.* **2013**, *33* (48), 18712−18727.
(31) Born, J.; Lange, T.; Kern, W.; McGregor, G. P.; Bickel, U.; Fehm, H. L. Sniffing neuropeptides: a transnasal approach to the human brain. *Nature neuroscience* **2002**, *5* (6), 514−516.
(32) Benedict, C.; Hallschmid, M.; Schmitz, K.; Schultes, B.; Ratter, F.; Fehm, H. L.; Born, J.; Kern, W. Intranasal insulin improves memory in humans: superiority of insulin aspart. *Neuropsychopharmacology* **2007**, *32* (1), 239−243.
(33) O'Doherty, D. P.; Bickerstaff, D. R.; McCloskey, E. V.; Atkins, R.; Hamdy, N. A.; Kanis, J. A. A comparison of the acute effects of subcutaneous and intranasal calcitonin. *Clin. Sci.* **1990**, *78*, 215−219.
(34) Chauhan, M. B.; Chauhan, N. B. Brain uptake of neurotherapeutics after intranasal versus intraperitoneal delivery in mice. *J. Neurol. Neurosurg.* **2015**, *2* (1), 9.
(35) Cattepoel, S.; Hanenberg, M.; Kulic, L.; Nitsch, R. M. Chronic intranasal treatment with an anti-Aβ30−42 scFv antibody ameliorates amyloid pathology in a transgenic mouse model of Alzheimer's disease. *PLoS One* **2011**, *6* (4), No. e18296.
(36) Kolobov, V.; Zakharova, I.; Fomina, V.; Gorbatov, V. Y.; Davydova, T. Effect of antibodies to glutamate on caspase-3 activity in brain structures of rats with experimental Alzheimer's disease. *Bulletin of experimental biology and medicine* **2013**, *154*, 425−427.
(37) Thorne, R.; Pronk, G.; Padmanabhan, V.; Frey, W., II Delivery of insulin-like growth factor-I to the rat brain and spinal cord along olfactory and trigeminal pathways following intranasal administration. *Neuroscience* **2004**, *127* (2), 481−496.
(38) Gudis, D.; Zhao, K.-Q.; Cohen, N. A. Acquired cilia dysfunction in chronic rhinosinusitis. *American journal of rhinology & allergy* **2012**, *26* (1), 1−6.
(39) Veronesi, M. C.; Alhamami, M.; Miedema, S. B.; Yun, Y.; Ruiz-Cardozo, M.; Vannier, M. W. Imaging of intranasal drug delivery to the brain. *Am. J. Nucl. Med. Mol. Imaging* **2020**, *10* (1), 1.
(40) Bleier, B. S. Novel topical therapeutics. *Otolaryngologic Clinics of North America* **2010**, *43* (3), 539−549. viii
(41) Costantino, H. R.; Illum, L.; Brandt, G.; Johnson, P. H.; Quay, S. C. Intranasal delivery: physicochemical and therapeutic aspects. *International journal of pharmaceutics* **2007**, *337* (1−2), 1−24.
(42) Shields, R. C.; Mokhtar, N.; Ford, M.; Hall, M. J.; Burgess, J. G.; ElBadawey, M. R.; Jakubovics, N. S. Efficacy of a marine bacterial nuclease against biofilm forming microorganisms isolated from chronic rhinosinusitis. *PLoS One* **2013**, *8* (2), No. e55339.
(43) Di Francesco, V.; Chua, A. J.; Davoudi, E.; Kim, J.; Bleier, B. S.; Amiji, M. M. Minimally invasive nasal infusion (MINI) approach for CNS delivery of protein therapeutics: A case study with ovalbumin. *J. Controlled Release* **2024**, *372*, 674−681.
(44) Padmakumar, S.; Jones, G.; Khorkova, O.; Hsiao, J.; Kim, J.; Bleier, B. S.; Amiji, M. M. Osmotic core-shell polymeric implant for sustained BDNF AntagoNAT delivery in CNS using minimally invasive nasal depot (MIND) approach. *Biomaterials* **2021**, *276*, No. 120989.

https://doi.org/10.1021/acsami.4c18679
ACS Appl. Mater. Interfaces 2024, 16, 69103−69113

(45) Chua, A. J.; Di Francesco, V.; D'Souza, A.; Amiji, M.; Bleier, B. S. Murine model of minimally invasive nasal depot (MIND) technique for central nervous system delivery of blood−brain barrier-impermeant therapeutics. *Lab Anim.* **2024**, *53*, 363−375.
(46) Chan, P. C.; Ramot, Y.; Malarkey, D. E.; Blackshear, P.; Kissling, G. E.; Travlos, G.; Nyska, A. Fourteen-week toxicity study of green tea extract in rats and mice. *Toxicologic pathology* **2010**, *38* (7), 1070−1084.
(47) Jeong, H.-K.; Jou, I.; Joe, E.-H. Systemic LPS administration induces brain inflammation but not dopaminergic neuronal death in the substantia nigra. *Experimental & molecular medicine* **2010**, *42* (12), 823−832.
(48) Skelly, D. T.; Hennessy, E.; Dansereau, M.-A.; Cunningham, C. A systematic analysis of the peripheral and CNS effects of systemic LPS, IL-1β, TNF-α and IL-6 challenges in C57BL/6 mice. *PloS one* **2013**, *8* (7), No. e69123.
(49) Zhao, J.; Wei, B.; Xiao, S.; Lan, X.; Cheng, X.; Zhang, J.; Lu, D.; Wei, W.; Wang, Y.; Li, H.; et al. Neuroinflammation induced by lipopolysaccharide causes cognitive impairment in mice. *Sci. Rep.* **2019**, *9* (1), 5790.
(50) Batista, C. R. A.; Gomes, G. F.; Candelario-Jalil, E.; Fiebich, B. L.; de Oliveira, A. C. P. Lipopolysaccharide-induced neuroinflammation as a bridge to understand neurodegeneration. *International journal of molecular sciences* **2019**, *20* (9), 2293.
(51) Zhang, J.; Xue, B.; Jing, B.; Tian, H.; Zhang, N.; Li, M.; Lu, L.; Chen, L.; Diao, H.; Chen, Y.; et al. LPS activates neuroinflammatory pathways to induce depression in Parkinson's disease-like condition. *Front. Pharmacol.* **2022**, *13*, No. 961817.
(52) Bittar, A.; Bhatt, N.; Kayed, R. Advances and considerations in AD tau-targeted immunotherapy. *Neurobiology of disease* **2020**, *134*, No. 104707.
(53) Ji, C.; Sigurdsson, E. M. Current status of clinical trials on tau immunotherapies. *Drugs* **2021**, *81* (10), 1135−1152.
(54) Mortada, I.; Farah, R.; Nabha, S.; Ojcius, D. M.; Fares, Y.; Almawi, W. Y.; Sadier, N. S. Immunotherapies for neurodegenerative diseases. *Frontiers in Neurology* **2021**, *12*, No. 654739.
(55) Cummings, J.; Osse, A. M. L.; Cammann, D.; Powell, J.; Chen, J. Anti-amyloid monoclonal antibodies for the treatment of Alzheimer's disease. *BioDrugs* **2024**, *38* (1), 5−22.
(56) Calabresi, P.; Mechelli, A.; Natale, G.; Volpicelli-Daley, L.; Di Lazzaro, G.; Ghiglieri, V. Alpha-synuclein in Parkinson's disease and other synucleinopathies: from overt neurodegeneration back to early synaptic dysfunction. *Cell Death Dis.* **2023**, *14* (3), 176.
(57) Robbins, M. Therapies for Tau-associated neurodegenerative disorders: targeting molecules, synapses, and cells. *Neural Regeneration Research* **2023**, *18* (12), 2633−2637.
(58) Craft, S.; Raman, R.; Chow, T. W.; Rafii, M. S.; Sun, C.-K.; Rissman, R. A.; Donohue, M. C.; Brewer, J. B.; Jenkins, C.; Harless, K.; et al. Safety, efficacy, and feasibility of intranasal insulin for the treatment of mild cognitive impairment and Alzheimer disease dementia: a randomized clinical trial. *JAMA Neurol.* **2020**, *77* (9), 1099−1109.
(59) Benedict, C.; Hallschmid, M.; Hatke, A.; Schultes, B.; Fehm, H. L.; Born, J.; Kern, W. Intranasal insulin improves memory in humans. *Psychoneuroendocrinology* **2004**, *29* (10), 1326−1334.
(60) Dhamoon, M. S.; Noble, J. M. Intranasal insulin improves cognition and modulates β-amyloid in early AD. *Neurology* **2009**, *72* (3), 292−294.
(61) Hallschmid, M. Intranasal insulin for Alzheimer's disease. *CNS drugs* **2021**, *35* (1), 21−37.
(62) Abbott, N. J. Blood−brain barrier structure and function and the challenges for CNS drug delivery. *Journal of inherited metabolic disease* **2013**, *36*, 437−449.
(63) Abbott, N. J.; Patabendige, A. A.; Dolman, D. E.; Yusof, S. R.; Begley, D. J. Structure and function of the blood−brain barrier. *Neurobiology of disease* **2010**, *37* (1), 13−25.
(64) Ballabh, P.; Braun, A.; Nedergaard, M. The blood−brain barrier: an overview: structure, regulation, and clinical implications. *Neurobiology of disease* **2004**, *16* (1), 1−13.
(65) Poduslo, J. F.; Curran, G. L.; Berg, C. T. Macromolecular permeability across the blood-nerve and blood-brain barriers. *Proc. Natl. Acad. Sci. U. S. A.* **1994**, *91* (12), 5705−5709.
(66) Felgenhauer, K. Protein size and cerebrospinal fluid composition. *Klinische Wochenschrift* **1974**, *52* (24), 1158−1164.
(67) Zhao, P.; Zhang, N.; An, Z. Engineering antibody and protein therapeutics to cross the blood−brain barrier. *Antibody Therapeutics* **2022**, *5* (4), 311−331.
(68) Bien-Ly, N.; Boswell, C. A.; Jeet, S.; Beach, T. G.; Hoyte, K.; Luk, W.; Shihadeh, V.; Ulufatu, S.; Foreman, O.; Lu, Y.; et al. Lack of widespread BBB disruption in Alzheimer's disease models: focus on therapeutic antibodies. *Neuron* **2015**, *88* (2), 289−297.
(69) Pardridge, W. M. Blood-brain barrier and delivery of protein and gene therapeutics to brain. *Front. Aging Neurosci.* **2020**, *11*, 373.
(70) Misra, A. *Challenges in delivery of therapeutic genomics and proteomics*; Elsevier, 2010.

https://doi.org/10.1021/acsami.4c18679
ACS Appl. Mater. Interfaces 2024, 16, 69103−69113